ChemComm

COMMUNICATION

View Article Online
View Journal

Cite this: DOI: 10.1039/c5cc03820k

Received 7th May 2015,
Accepted 16th June 2015

DOI: 10.1039/c5cc03820k

www.rsc.org/chemcomm

Photopolymerized micelles of diacetylene amphiphile: physical characterization and cell delivery properties†

Patrick Neuberg,‡[ab] Aurélia Perino,‡[a] Emmanuelle Morin-Picardat,‡[ab] Nicolas Anton,[c] Zeinab Darwich,[d] Denis Weltin,[e] Yves Mely,[d] Andrey S. Klymchenko,[d] Jean-Serge Remy*[b] and Alain Wagner*[a]

A series of polydiacetylene (PDA) – based micelles were prepared from diacetylenic surfactant bearing polyethylene glycol, by increasing UV-irradiation times. These polymeric lipid micelles were analyzed by physicochemical methods, electron microscopy and NMR analysis. Cellular delivery of fluorescent dye suggests that adjusting the polymerization state is vital to reach the full *in vitro* potential of PDA-based delivery systems.

Among the great diversity of nanoparticles, PDA-based micelles recently appeared as very promising vectors for drug delivery. Pioneering work has been done by Eric Doris' group using highly polymerized PDA-micelles as enhanced drug loading systems with promising pharmacodistribution profiles.[1] PDA-based micelles are spherical objects of 5–10 nm diameter made by photopolymerization of surfactants bearing hydrophobic chain of 12–20 carbon atoms, a polar head group and a photopolymerizable diacetylenic motif.[2] Our previous studies showed that photopolymerization stabilizes the structure of PDA-based micelles bearing a highly polar nitriloacetic acid (NTA) polar head but do not alter their shape neither their morphology. Varying the polar head group, we also studied cationic PDA-based micelles, which showed remarkable gene delivery properties.[3] More recently, Doris *et al.* extended work on PDA-based micelles evaluating their potential for *in vivo* drug delivery.[4–6] Only highly polymerized micelles were used in these studies, and little is known about how the polymerization level impacts the aforementioned delivery potential and their biological delivery activities. To fill this gap, we report herein to which extent the photopolymerization of the PDA-based micelles lowers their cytotoxicity and how it impacts their delivery efficiency of hydrophobic drugs. Interaction of polymeric micelles with living cells and intracellular delivery were recently studied by intracellular tracking of fluorescently labelled micelles,[5,7] either by covalently linking the dye on the micelles,[8–10] or by inserting an apolar dye in the hydrophobic domain of the micelles.[11,12] In the present study, we tested the delivery of a hydrophobic fluorescent probe based on Nile Red dye chemically modified with a lipid anchor group (NR12S).[13,14] This probe turns on its fluorescence upon binding to lipid membranes and shows selective staining of the cell plasma membranes. Since NR12S alone cannot internalize rapidly inside the cells, its encapsulation in micelles allowed us to evaluate the delivery potential ability of the polymerized micelle to reach the cytoplasm.

The non-polymerized micelles (NPM) were obtained by self-assembly of amphiphile **1** (Fig. 1) in phosphate buffer pH 7.4. NPMs were further exposed to an UV-irradiation at 254 nm (48 W lamp), in order to obtain polymerized micelles (PM). The photopolymerization was studied by UV-spectroscopy for irradiation times of 30 min, 1 h, 2 h, 4 h and 8 h. Non-polymerized lipid (NPM) only shows weak absorption from 200 to 300 nm (see ESI,† Fig. S1). After 30 minutes of irradiation, the solution turned yellow and absorption peaks appeared at longer wavelengths (300–400 nm), indicating the formation of conjugated ene–yne systems.

At 4 hours of irradiation, the UV absorption was the highest, indicating maximum polymerization. At longer irradiation times (8 hours) the conjugated system progressively degraded. This reported phenomenon is generally explained by polymer photobleaching,[15–17] which creates defects in the ene–yne backbone.

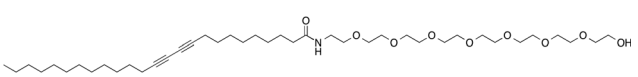

Fig. 1 Structure of surfactant **1**.

[a] *Laboratory of Functional Chemo Systems, and Labex Medalis, CAMB, UMR 7199 CNRS, Faculty of Pharmacy, University of Strasbourg, 74 route du Rhin, 67401 Illkirch, France. E-mail: alwag@unistra.fr*

[b] *Laboratory V-SAT, Vectors – Synthesis and Therapeutic Applications, and Labex Medalis, CAMB, UMR 7199 CNRS, Faculty of Pharmacy, University of Strasbourg, 74 route du Rhin, 67401 Illkirch, France. E-mail: remy@unistra.fr*

[c] *Laboratory of Biogalenic Pharmacy, CAMB, UMR 7199 CNRS, Faculty of Pharmacy, University of Strasbourg, 74 route du Rhin, 67401 Illkirch, France*

[d] *Laboratory of Biophotonic and Pharmacology, UMR 7213, Faculty of Pharmacy, University of Strasbourg, 74 route du Rhin, 67401 Illkirch, France*

[e] *Phytodia SAS, Boulevard Sébastien Brant, 67412 Illkirch, France*

† Electronic supplementary information (ESI) available: Experimental detail for the synthesis of **1** and characterisation of the micelles, DOSY-NMR data, experimental detail on cell delivery of fluorescent probe. See DOI: 10.1039/c5cc03820k

‡ These authors contributed equally.

The sizes of the micelles were measured by dynamic light scattering (DLS; ESI,† Fig. S1) and by transmission electron microscopy (TEM; ESI,† Fig. S2).

For NPM and PM, the measured hydrodynamic diameter was almost identical whatever the polymerization time, comprised between 9 and 10 nm (DLS; see ESI,† Fig. S3) and of spherical shape (TEM).

We measured how photopolymerization impacts on the surface tension of these diacetylenic lipids micelles, giving information on their internal organization. Dynamic surface tension was measured with a Tracker® drop tensiometer, according to the axisymmetric drop shape analysis. The droplet shape was recorded in real time with a video camera. As a result, the Laplacian shape of the drop gives its interfacial area and surface tension. Measurements were followed up until stabilization of the surface tension. We compared the same samples with (8 h) and without irradiation (red and blue curves in Fig. 2, respectively). The results showed that irradiation strongly affects the surface-active properties of the solutions. Stabilization times of irradiated solutions were increased while the effect on surface tension was reduced. This is fully coherent with a loss of surfactant properties of the molecules upon the irradiation process. That is to say the remaining monomeric surfactant molecules in the polymerized micelles are less abundant and less prone to migrate to the interfaces, affecting the surface properties of the solution. From these experiments, we deduced experimental CMC values (Fig. 2). NPM showed CMC of 3.5 μg mL^{-1} while PM showed higher CMC values (16.3 μg mL^{-1}). This surprising increase of the measured CMC of polymerized surfactant directly reflects the decrease in monomer surfactant concentration, as polymerized lipid does not contribute to the lowering of surface tension. Thus, we can deduce from the ratio of the CMC values of NPM and PM that around 20% ($CMC_{(NP)}$/$CMC_{(PM)}$ × 100%) of total lipid was still non-polymerized even at extended UV irradiation times (8 hours).

Polymerized and non-polymerized solutions of surfactant **1** were then analysed by DOSY NMR experiments (diffusion ordered NMR spectroscopy) in deuterated water. Applying the Stokes Einstein relation for the diffusion of spherical particles through a liquid, their hydrodynamic radii were calculated from the measured diffusion coefficients and were in full accordance with the DLS experiments. DOSY experiments of the non-polymerized surfactant on the other hand showed high diffusion rates in deuterated methanol as expected for a free molecule in solution (see ESI† for details).

We used the dissociation of surfactant molecules in methanol to further analyse polymerized micelles by DOSY experiments. Polymerized micelles (4 h irradiation in water solution) were lyophilized and then dissociated again in deuterated methanol. Subpopulations of polymerized surfactant and monomeric surfactant molecules could then be detected by DOSY analysis of total solute in methanol (Fig. 3). The DOSY analysis of the surfactant solution in methanol revealed two distinct populations: one corresponding to free molecules (with diffusion coefficient D = 629 10^{-12} m^2 s^{-1}), the second corresponding to polymerized surfactant with a low diffusion coefficient (diffusion coefficient D = 141 10^{-12} m^2 s^{-1}). The percentage of covalently bridged surfactant *versus* monomer lipids could be calculated from peak integration from the 3D-plot. At 4 hours UV-polymerization we measured a total of 75% polymerized surfactant compared to 25% remaining monomeric form, in accordance with our surface tension experiments (for detailed DOSY analysis see ESI†).

We further studied the incorporation of a fluorescent membrane probe NR12S into these micelles at various levels of polymerization.

NR12S is poorly fluorescent in water, while it becomes highly fluorescent when bound to lipid structures.[13] The fluorescence intensity of the dye incorporated into micelles increased with the dye concentration (up to 1–2 μM) for both NPM and PM (Fig. 5). Above 1–2 μM, the intensity of the probe saturated and further dropped. Importantly, increasing the photopolymerization time of micelles leads to a decrease of the probe concentration at which the saturation effect was observed. This clearly shows that higher photopolymerization times decrease the capacity of the micelles to incorporate the probe. It is likely that the polymerized micellar core exhibits a decreased number of probe binding sites. Moreover the emission band of NR12S slightly shifted to the blue for the higher photopolymerization times. As this dye is

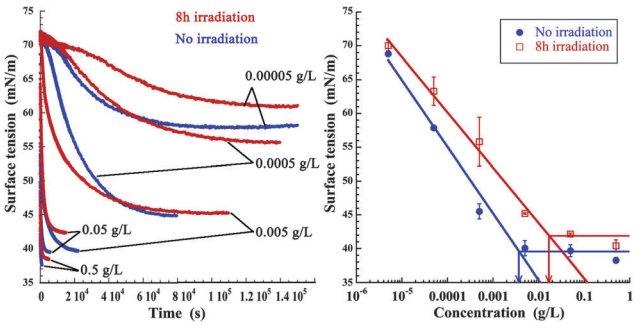

Fig. 2 Dynamic surface tension measurements at various concentrations of non-polymerized (blue) and polymerized micelles (red) (left), and plot of surface tension at equilibrium at various concentrations of non-polymerized and polymerized micelles (right).

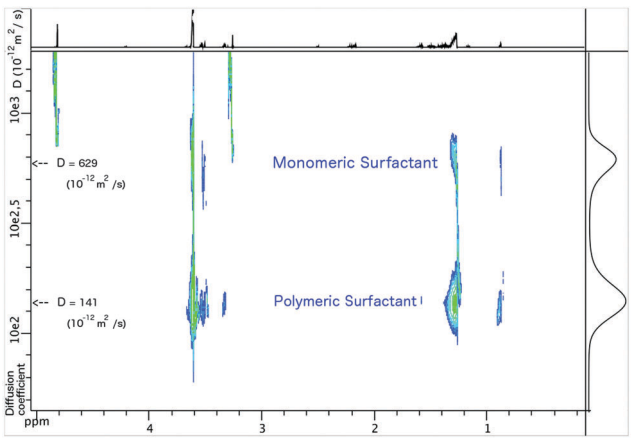

Fig. 3 DOSY NMR analysis of polymerized micelle (4 hour polymerization) after lyophilisation and suspension in deuterated methanol.

solvatochromic,[13] this blue shift indicates that in polymerized micelles the binding sites are less polar.

We could speculate that at higher photopolymerization times the packing of the detergent molecules within the micelles is tighter, which leads to the observed decrease in the local polarity values.

Micelles labelled with NR12S were further studied by Fluorescence Correlation Spectroscopy (FCS; see ESI,† Table S4). The observed correlation time for the labelled particles was rather uniform for NPMs and PMs, corresponding to the hydrodynamic diameters of 8.5–9.1 nm (see ESI,† Table S4), in line with the DLS and TEM data, and further confirming that the size of the particles is independent of photopolymerization time. Moreover, our data also indicate that the dye does not affect the particle diameter, which was expected because of its use at 1/50 (dye/surfactant) molar ratio. The brightness of the particles was moderately decreased for higher polymerization times (2–8 hours; Fig. 4), in line with observed lower capacity of the micelles to bind NR12S probe. Probe NR12S was designed to bind exclusively the outer leaflet of cell membranes without rapid internalization through the lipid bilayers.[13] We wanted to understand whether the polymerized micelles can help the probe to cross the membrane barriers and to internalize inside the cells. For this purpose, live cells were incubated with probe-loaded micelles for various times and studied by fluorescence microscopy. Early after addition of labelled micelles (polymerized for 30 minutes) or NR12S alone, the cells showed fluorescence localized exclusively at the plasma membrane (Fig. 5). After incubation time beyond 1 h with the micelles, a diffuse fluorescence was observed all over the cytosol, while the nucleus remained unstained. In contrast, when the cells were incubated only with NR12S, intracellular dots were detected, which is a typical signature of endosomes that probably recruited the probe bound to the cell membrane.[14] Thus, it appears that the micelles change the internalization pathway of the probe and help it to cross the membrane barriers. Remarkably, the efficiency of the micelles to deliver the NR12S probe into the cytoplasm depends drastically on their photopolymerization time. Indeed, NPM showed the most efficient delivery of NR12S into the cytosol as the intracellular fluorescence was the brightest after 4 h of incubation with these micelles (Fig. S2, ESI†). The intracellular fluorescence decreases with the increase in the photopolymerization time. In the case of PM for 4 and 8 h, the images were very similar to the control experiments using only NR12S, indicating that highly photopolymerized micelles cannot deliver the probe across the membrane barriers. These polymeric nanostructures are probably unable

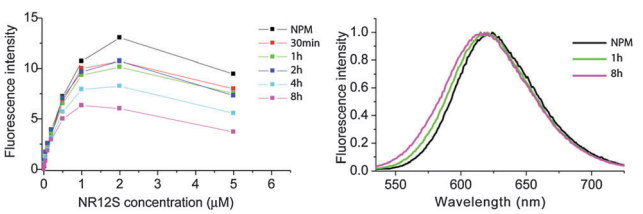

Fig. 4 Titration of micelles at various polymerization times with probe NR12S. Surfactant **1** concentration was 0.05 mg mL^{-1} (60 μM), in phosphate buffer.

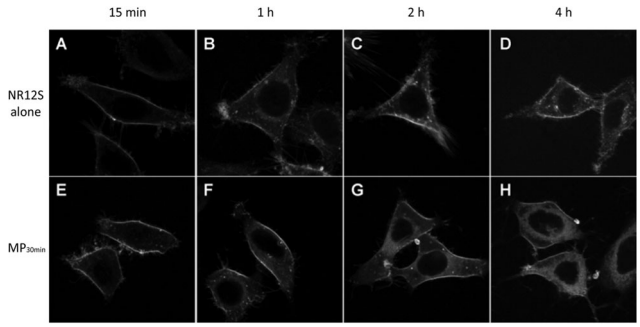

Fig. 5 Fluorescence images of HeLa cells incubated at 37 °C with NR12S dye alone (A–D) and incorporated in micelles (E–H) (polymerized for 30 min). Incubation times were: 15 min (A, E), 1 h (B, F), 2 h (C, G) and 4 h (D, H).

to interact and destabilize lipid bilayers, which can be related to their much higher stability. It is known from the field of gene delivery that lipid based non-viral vectors deliver DNA into the cytosol by using mechanisms of membrane destabilization.[18] In parallel, polymer-based vectors deliver DNA by an alternative mechanism, related to proton sponge effect.[19,20] Here, we observe something similar, as the efficiency of probe delivery decreases when the micelles change from lipid-based to polymeric. Nevertheless, the micelles polymerized for 30 min–2 h preserve their ability to deliver the probe, indicating that these conditions are optimal for cellular-delivery applications.

Finally, the cytotoxicity of surfactant **1** and its polymerized micelles, irradiated for various times, was verified *in vitro* on HaCaT cell line (ESI,† Fig. S7). The non-polymerized sample of **1** was toxic at concentrations ≥ 25 μg mL^{-1} (IC_{50} = 25 μg mL^{-1}). The observed toxicity of monomeric surfactant is in line with a recent comparative study of C25 diacetylenic lipoamine surfactants which are described as being more cytotoxic than their saturated C25 chain analogues (N. Ménard 2012).[21] The cytotoxicity of surfactant **1** dropped rapidly with the photopolymerization time of the micelles. Thus, for 30 min of photopolymerization, the sample was toxic at concentrations ≥ 100 μg mL^{-1}, while for 8 h of polymerization, cytotoxicity was not observed, even for the highest concentration used (200 μg mL^{-1}). This observation of decrease of cytotoxicity with UV irradiation times of the micelles correlate with the degree of conversion of monomeric lipid to polymeric surfactants. Thus, polymerized micelles made of multimeric amphiphiles show lower cytotoxicity than micelles made of monomeric surfactants.

These results correlate well with the data on the ability of the micelles to assist the delivery of NR12S probe, so that the non-polymerized sample of **1**, which is the most efficient agent for NR12S delivery, is also the most toxic. We can speculate that the cytotoxicity of **1** is probably linked with its ability to destabilize cell membranes and enter the cytosol, because monomeric form of **1** exhibits stronger surfactant properties than its polymerized multimeric forms. Importantly, micelles with medium level of polymerization (30 min–2 h) show much lower cytotoxicity compared to non-polymerized sample, while preserving their ability to deliver the probe, which make them prospective as delivery agents for nonpolar molecules that cannot enter the cells.

Recent work describes the synthesis of small crosslinked PDA nanovesicles based on a co-formulation of pentacosadiynoic acid with neutral PEGylated lipids for sustained drug release.[21] Fine control of the size of these nanovesicles was achieved ranging from 40 to 200 nm.[22] The PDA micelles on the other hand are even smaller (*ca.* 10 nm) than classical block co-polymer micelles. Their small size, according to Doris *et al.*, allows for deeper diffusion into target tissues and stronger tumour accumulation due to EPR effect (enhanced permeability and retention effect).[4] Our results show that fine-tuning of the photopolymerization level in PDA micelles can decrease their cytotoxicity, while preserving efficient intracellular delivery of an encapsulated compound. This opens up new ways to prepare improved PEGylated micelles-based drug delivery agents by functionalization of the nanocarrier with targeting ligands to enhance tissue selectivity and fine-tuned polymerization to keep low cytotoxicity and enhance intracellular delivery efficacy.

This work shows the study of PEGylated polydiacetylene micelles, and their potential use as tools for drug delivery. Photopolymerization leads to more stable structures without structural or morphological changes. High polymerization times lead to incomplete polymerization of lipids, with remaining unchanged monomer surfactant. The loading capacity, the intracellular delivery of a hydrophobic fluorescent probe (NR12S) by micelles and their cytotoxicities are strongly influenced by the photopolymerization degree. It thus appears that adjusting micelles polymerization enables fine-tuning of the intracellular delivery/cytotoxicity ratio. The micelles obtained after short irradiation times seem to be a good compromise between efficiency and toxicity for delivery applications.

This work was supported by the French government (MESR), the Région Alsace, the LABEX MEDALIS, icFRC, CNRS and the ANR JCJC (ANR-11-JS07-014-01). The authors would like to thank Christine Ruhlmann from the IGBMC for her help with TEM, Cyril Antheaume and Justine Vieville from Chemical Analysis Service Platform at Faculty of Pharmacy at Strasbourg University. Applications, and Labex Medalis, CAMB, UMR7199 CNRS, Faculty of Pharmacy, University of Strasbourg, 74 route du Rhin, 67401 Illkirch (France).

Notes and references

1 J. Ogier, T. Arnauld, G. Carrot, A. Lhumeau, J.-M. Delbos, C. Boursier, O. Loreau, F. Lefoulon and E. Doris, *Org. Biomol. Chem.*, 2010, **8**, 3902–3907.
2 A. Perino, A. Klymchenko, A. Morere, E. Contal, A. Rameau, J.-M. Guenet, Y. Mély and A. Wagner, *Macromol. Chem. Phys.*, 2011, **212**, 111–117.
3 E. Morin, M. Nothisen, A. Wagner and J.-S. Remy, *Bioconjugate Chem.*, 2011, **22**, 1916–1923.
4 N. Mackiewicz, E. Gravel, A. Garofalakis, J. Ogier, J. John, D. M. Dupont, K. Gombert, B. Tavitian, E. Doris and F. Ducongé, *Small*, 2011, **7**, 2786–2792.
5 E. Gravel, B. Thézé, I. Jacques, P. Anikumar, K. Gombert, F. Ducongé and E. Doris, *Nanoscale*, 2013, **5**, 1955–1960.
6 E. Gravel, J. Ogier, T. Arnauld, N. Mackiewicz, F. Ducongé and E. Doris, *Chemistry*, 2012, **18**, 400–408.
7 J. You, F.-Q. Hu, Y.-Z. Du and H. Yuan, *Biomacromolecules*, 2007, **8**, 2450–2456.
8 R. Savic, L. Luo, A. Eisenberg and D. Maysinger, *Science*, 2003, **300**, 615–618.
9 A. Papagiannaros, A. Kale, S. T. Levchenko, D. Mongayt, W. C. Hartner and V. P. Torchilin, *Int. J. Nanomed.*, 2009, **4**, 123–131.
10 D.-Q. Wu, B. Lu, C. Chang, C.-S. Chen, T. Wang, Y.-Y. Zhang, S.-X. Cheng, X.-J. Jiang, X.-Z. Zhang and R.-X. Zhuo, *Biomaterials*, 2009, **30**, 1363–1371.
11 A. Mahmud and A. Lavasanifar, *Colloids Surf., B*, 2005, **45**, 82–89.
12 W.-C. Wu, C.-Y. Chen, Y. Tian, S.-H. Jang, Y. Hong, Y. Liu, R. Hu, B. Z. Tang, Y.-T. Lee, C.-T. Chen, W.-C. Chen and A. K. Y. Jen, *Adv. Funct. Mater.*, 2010, **20**, 1413–1423.
13 O. A. Kucherak, S. Oncul, Z. Darwich, D. A. Yushchenko, Y. Arntz, P. Didier, Y. Mély and A. S. Klymchenko, *J. Am. Chem. Soc.*, 2010, **132**, 4907–4916.
14 Z. Darwich, A. S. Klymchenko, D. Dujardin and Y. Mély, *RSC Adv.*, 2014, **4**, 8481–8488.
15 C. F. Temprana, E. L. Duarte, M. C. Taira, M. T. Lamy and S. del Valle Alonso, *Langmuir*, 2010, **26**, 10084–10092.
16 S. M. Daly, L. A. Heffernan, W. R. Barger and D. K. Shenoy, *Langmuir*, 2005, **22**, 1215–1222.
17 K. Ogawa, *J. Phys. Chem.*, 1989, **93**, 5305–5310.
18 L. Wasungu and D. Hoekstra, *J. Controlled Release*, 2006, **116**, 255–264.
19 W. Zauner, M. Ogris and E. Wagner, *Adv. Drug Delivery Rev.*, 1998, **30**, 97–113.
20 O. Boussif, F. Lezoualc'h, M. A. Zanta, M. D. Mergny, D. Scherman, B. Demeneix and J.-P. Behr, *Proc. Natl. Acad. Sci. U. S. A.*, 1995, **92**(16), 7297–7301.
21 N. Ménard, N. Tsapis, C. Poirier, T. Arnauld, L. Moine, F. Lefoulon, J.-M. Péan and E. Fattal, *Int. J. Pharm.*, 2012, **423**, 312–320.
22 C. Guo, L. Zeng, S. Liu, Q. Chen, Z. Dai and X. Wu, *J. Nanosci. Nanotechnol.*, 2012, **12**, 245–251.

